

PROBABILISTIC MODELLING OF STORM WAVE CLUSTERING AT OLD BAR, NSW, INCLUDING THE IMPACTS OF SEASONAL AND ENSO CYCLES

G Davies¹, D P Callaghan², U Gravois², D Hanslow³, W Jiang¹, S Nichol¹, T Baldock²

¹Geoscience Australia, Canberra, ACT

²University of Queensland, St Lucia, QLD

³Office of Environment and Heritage, Newcastle, NSW

Abstract

Historically, coastal erosion has caused significant property and infrastructure damage in NSW. Extreme erosion can be caused by individual storms, or by multi-storm ‘clusters’ which may induce disproportionate erosion relative to their size. Additionally, potentially significant changes in storm wave properties may occur in association with seasonal and ENSO (El Niño-Southern Oscillation) cycles, with several studies finding that ENSO affects the mean shoreline position and likelihood of extreme erosion in NSW.

Quantification of site-specific erosion hazards is necessary to support coastal management. Probabilistic approaches are attractive because they avoid reliance on arbitrarily chosen ‘design’ events, and provide more complete information on both the range and likelihood of erosion. Callaghan et al. (2008) developed a methodology for probabilistic erosion hazard assessment on sandy shorelines, combining a probabilistic model of storm waves with a deterministic shoreline evolution model. The probability of the shoreline eroding past a given position (over a given timeframe) may be quantified, and uncertainties associated with, for example, our limited knowledge of the frequency of very large storms, are accounted for with bootstrapping.

Herein we develop a probabilistic model of the storm wave climate at Old Bar, NSW, for use in coastal erosion hazard assessment. The statistical method of Callaghan et al. (2008) is extended to account for the impacts of ENSO and seasonality on storm wave properties and storm frequency. On average, storm wave properties (height, duration, period, surge, mean sea level (MSL)) are of greater magnitude in winter than summer, and during La Niña the MSL and rate of storms is higher, and the wave direction becomes more easterly, compared with El Niño. Ongoing work is modelling the shoreline response to these conditions at Old Bar.

A contribution to Bushfire and Natural Hazards CRC Project “Resilience to clustered disaster events on the coast – storm surge”.

Introduction

On the wave dominated sandy shorelines of New South Wales, coastal erosion has historically had significant impacts on the built environment and coastal amenity (Kinsela and Hanslow, 2013), with the well-publicised erosion of Narrabeen beach in June 2016 being a significant recent example. To support management of these risks, probabilistic models of shoreline retreat are needed to quantify coastal erosion hazards (e.g. Cowell et al., 2006; Hanslow et al., 2016; Kinsela et al., 2016; Wainright et al., 2015) and provide input for detailed cost-benefit analysis of management options. One popular approach to modelling coastal erosion hazards involves combining deterministic shoreline

evolution models with stochastic storm wave boundary conditions (e.g. Callaghan et al., 2008, 2013; Corbella and Stretch 2012; Li et al., 2014; Ranasinghe et al., 2012). With this approach, a large suite of monte-carlo shoreline evolution time-series are simulated to approximate the distribution of future shoreline positions (or equivalently, the probability of erosion) over a given time-horizon. Realistic modelling of the stochastic storm wave forcing is a crucial aspect of this approach, because it gives rise to stochasticity in the future shoreline position and controls the variability of the latter (an alternative approach to treating these uncertainties, not considered herein, is to directly model the variability in sediment fluxes without modelling waves, see e.g. Cowell et al., 2006; Kinsela et al., 2016). In the current study we focus on the development of realistic stochastic storm wave event sequences which can be used to force shoreline evolution models (Callaghan et al., 2013). The aim is to develop a framework which allows seasonal and climatic (e.g. ENSO) non-stationarities in the wave climate to be accounted for in coastal erosion hazard assessments.

Beach erosion during storms is known to be affected by the pre-storm beach morphology as well as the storm wave height, duration, wave period, wave direction, tide and surge (Coco et al., 2014). The sequencing of consecutive storms can significantly affect erosion (Southgate, 1985), and closely spaced storm events (often termed 'storm clusters') can potentially induce disproportionate erosion relative to their size (Ferreira, 2005; Dissanayake et al., 2015). Storm clustering was recognised as far back as 1974 as being a significant contributor to several severe erosion events in NSW (Thom 1974). The need to simulate shoreline erosion has thus driven considerable research on multivariate statistical modelling of synthetic storm sequences, with particular focus on the simulating dependence in the storm wave properties (Callaghan et al., 2008; Li et al., 2014b; de Michele et al., 2007). Less attention has been given to adapting such models to include non-stationarities in the storm properties associated with, for example, climatic and seasonal cycles (Serafin and Ruggiero, 2014).

However, a number of studies suggest that non-stationarities have a strong effect on both storm wave climate and shoreline erosion in many locations, including on the New South Wales coast (e.g. Barnard et al., 2015; Harley et al., 2010; Harley et al., 2011; Ranasinghe et al., 2004; You and Jayewardene, 2003; You and Lord, 2008). For example, Barnard et al. (2015) examined the relationships between shoreline evolution, wave climate and large scale climate indices at a 48 beaches throughout the Pacific Ocean basin, and concluded that coastal vulnerability is dominated by the El Nino-Southern Oscillation. While the significance of such non-stationarities may vary from site-to-site, it is clearly important to have general techniques available to integrate them into erosion hazard assessments.

Herein we present a methodology for integrating seasonal and ENSO related non-stationarities into probabilistic models of storm wave climate, which facilitates the inclusions of such non-stationarities in erosion hazard assessments. The model is applied to Old Bar, an erosion hotspot in NSW with a history of significant erosion related property damage. The integration and processing of wave and tidal datasets relevant to Old Bar is discussed in the next section, followed by an exploratory analysis of the influence of seasonal and ENSO non-stationarities on the storm wave climate. We finally outline the statistical modelling framework, with particular focus on the model's representation of seasonal and ENSO related non-stationarities in the storm events.

Study Site and Data Processing

The Old Bar beach-dune system is situated on the mid-north coast of New South Wales (Figure 1). The coastline faces south-east and is open to the predominately south-easterly wave climate. The beach morphodynamic type is intermediate, with a typical state characterised by a double-bar system, including a sequence of rips which intersect the inner bar and locally erode the beach face (Nichol et al., 2016). Backing the beach is a continuous dune system featuring a number of beachfront properties. Erosion of the dune face in the central section of the Old Bar embayment has resulted in the loss of some properties and infrastructure damage since the 1970's, with a number of existing properties threatened by ongoing erosion (Figure 1; Kinsela and Hanslow, 2013; Nichol et al., 2016).

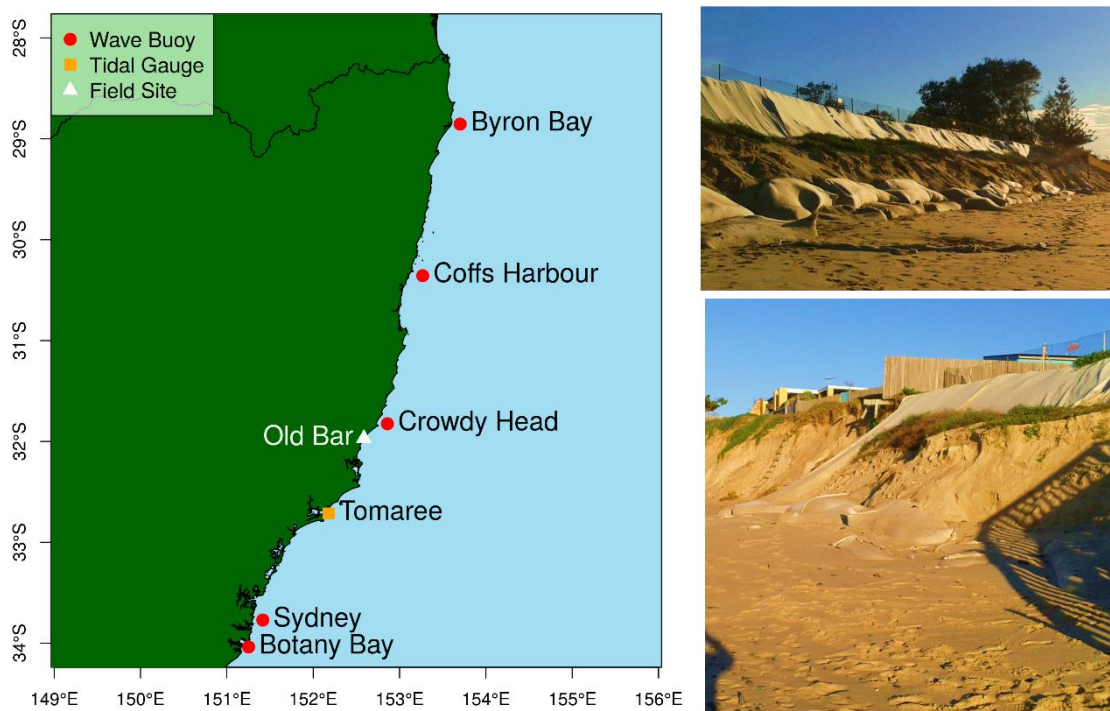


Figure 1: (Left) Location of Old Bar, along with the nearby waverider buoys, and the Tomaree tidal gauge. (Right) Shoreline erosion threatening coastal properties at Old Bar.

To develop a time-series of wave observations relevant to Old Bar, hourly wave statistics (significant wave height, wave direction and wave period) were obtained from Manly Hydraulics Laboratory for waverider buoys at Crowdy Head, Coffs Harbour and Sydney (Figure 1; Kulmar et al., 2013). The hourly wave period and direction are defined as the period and direction of the peak of the wave energy spectrum. The Crowdy Head waverider buoy was the preferred data source for representing wave conditions at Old Bar. At this site wave data covers the period October 1985 – January 2016 with some gaps due to instrument malfunction. Data from other waverider buoys was used to fill gaps in the Crowdy Head wave time-series, as explained below.

Tidal data was obtained from the Tomaree tidal gauge (Figure 1), and was separated into astronomical and non-astronomical components using astronomical tidal predictions from TPX07.2 (Egbert and Erofeeva, 2002). The non-astronomical tidal component was

further decomposed into: 1) a smooth inter-annual MSL trend; 2) an annually periodic monthly MSL component, and; 3) a residual which reflects storms and other relatively short term oceanographic processes like shelf waves (this residual is termed the ‘surge’ henceforth). This was achieved using the Seasonal-Trend-Loess algorithm, which is a standard technique for time-series decomposition (Cleveland et al., 1990).

The Crowdy Head hourly wave time-series had an 87% data capture rate from October 1985 to January 2016, except for wave direction which was measured since 2011. To simplify the data analysis, a single nearly-continuous “Old Bar” time-series was created by filling gaps in the Crowdy Head data with contemporaneous measurements at the Coffs Harbour and Sydney waverider buoys (in order of preference). Because wave direction has only been measured at Sydney since 1992 and at Coffs harbour since 2012, hindcast wave directions for Sydney based on synoptic weather charts (Kulmar, 1995) were also used for gap-filling if no measured data was available. The final gap-filled time-series was largely complete in significant wave height (99%), while tidal stage was 92% complete, and wave direction was 87% complete. Excluding wave direction, the wave statistics in this gap-filled time-series were largely sourced from Crowdy Head (87%) and Coffs Harbour (11%). Most (52%) of the wave direction measurements originated from the Sydney waverider buoy, while 32% originated from the hindcast Sydney wave directions, and the remainder largely originated from Crowdy Head (14%). This heterogeneity led to spurious non-stationarities in the gap-filled wave-direction series which were removed as described below.

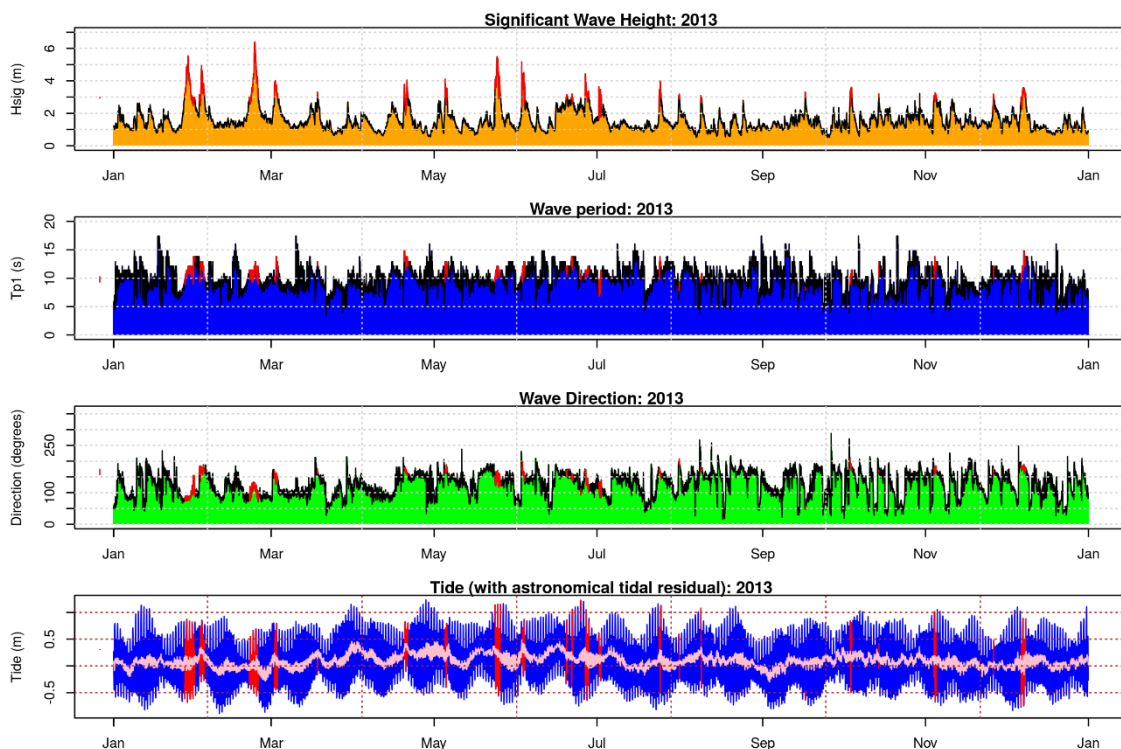


Figure 2: Storm events for Old Bar extracted from the gap-filled time-series of waves and tides. Only the year 2013 is depicted, although the data covers October 1985 – January 2016. Red overplotting is used to denote the storm events, which were identified with a peaks-over-threshold approach as described in the text. The top panel gives the hourly significant wave height. The second panel gives the wave period. The third panel gives the wave direction (degrees from north). The bottom panel gives the tide (blue) and the non-astronomical tidal component

(pink) derived by subtracting astronomical tidal predictions from the observations.

Our analysis required distinguishing discrete storm events from the continuous time-series of wave statistics. This was achieved using a peaks-over-threshold methodology (Figure 2). Initially we identified all time periods where the significant wave height continuously exceeded a threshold of 2.92m (the latter being the 95th percentile of the entire significant wave height time-series). Each continuous threshold-exceedance was treated as a distinct preliminary storm event. Finally, the preliminary storm events were merged if they were separated in time by less than 24 hours (Figure 2). This merging removed statistically significant auto-correlations from the storm event summary statistics, which serves to simplify the statistical modelling.

For each storm event we then extracted the event start time and a set of five summary statistics $\{H_{sig}, R, D, T, \theta\}$ (defined below) which are the focus of the subsequent analysis (Figure 3). If the data required to compute a particular summary statistic for a particular event was missing (e.g. due to missing tidal or wave direction data), then that statistic was treated as missing data.

- H_{sig} was defined as the peak significant wave height (m) during the event.
- R was defined as the peak surge (m) during the event.
- D was defined as the time difference (hours) between the first and last event observation plus one hour (to ensure that events consisting of only one observation are treated as having one hour duration, consistent with the hourly resolution of the data).
- T was defined as the wave period (s) at the time of peak significant wave height.
- θ was defined as the wave direction (degrees) derived from the wave direction at the time of peak significant wave height, with a bias correction applied depending on the site from which the data originated.

Preliminary analysis showed that gap-filled storm directions originating from the Sydney hindcasts were on average more easterly than those originating from the Sydney waverider (see also Kulmar, 1995), while the latter were on average more easterly than the storm directions originating from Coffs Harbour and Crowdy Head. To reduce these unwanted site related inhomogeneities, a quantile-matching transformation was applied to make the storm direction data from each station have a distribution more similar to that measured at Crowdy Head. While details of this transformation are provided below, and their effect is shown in Figure 3, it is important to note that the qualitative relations between ENSO, seasonality and wave direction discussed in this study occur irrespective of whether or not the quantile matching transformation is applied. However, because the bias correction leads to a general southward shift in the wave direction distribution (Figure 3), the quantitative details of the relationships are affected.

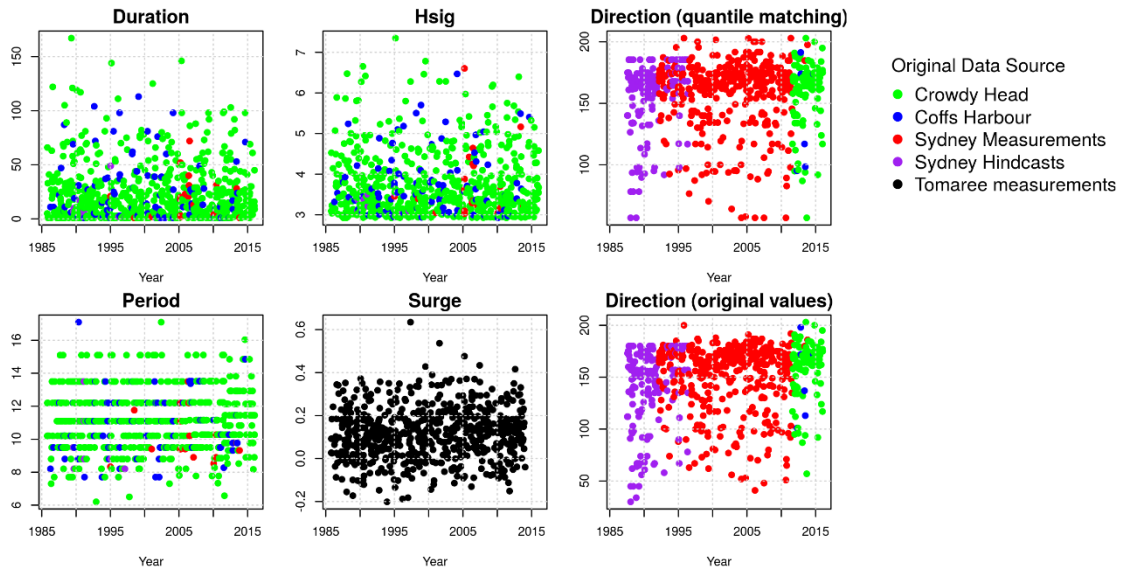


Figure 3: Time-series of the Old Bar storm summary statistics, coloured by the station from which the original data was obtained. For comparison we show both the original (raw) storm directions, as well as the storm directions following the quantile-matching bias correction. The latter were used for the analysis because of the strong inhomogeneities in the original values, which are caused by the combination of data from different sources.

The storm direction quantile matching transformation was derived by first identifying the time of peak H_{sig} during all storm events defined above. At each of those times we extracted the wave direction for every station separately. For each station we then created a piecewise linear function $F_{station}(\theta) \rightarrow [1/(N+1), N/(N+1)]$ which interpolates between the sorted storm directions and their empirical non-exceedance probabilities $r_{\{i\}}/(N+1)$, where $r_{\{i\}}$ is the rank of the i th wave direction sorted in increasing order, and N is the number of non-missing directions extracted from the station. Repeated direction values (ties) were assigned the same mean rank $r_{\{i\}}$. The quantile-matching transformation involved applying $F_{station}$ to all the storm direction data which originated from the corresponding station, followed by application of the inverse of F_{Crowdy_Head} . This ensured that quantiles of the transformed storm direction data from each station were similar to corresponding quantiles at Crowdy Head (Figure 3). One limitation of the approach is the occurrence of repeated maximum and minimum values in some transformed wave directions (Figure 3). These occur partly because of ties in the original directions (repeated values of 180 degrees), and also because the Sydney stations have more measured wave directions (larger N) than the Crowdy Head station, which implies that for Sydney stations $F_{station}$ covers a slightly larger range than F_{Crowdy_Head} . Therefore, application of our quantile matching transformation sometimes requires extending the inverse of F_{Crowdy_Head} to values slightly outside its original domain. The nearest maximum or minimum Crowdy Head storm direction was assigned to such cases, which leads to some repeated values at extremes of direction (Figure 3). As noted above, the qualitative relations we report between ENSO, seasonality and wave direction occur irrespective of whether this adjustment is applied.

Exploratory analysis of non-stationarities in the storm wave properties

All the storm summary statistics exhibit seasonal non-stationarities in their distributions, as does the overall rate of storm events (Figure 4). There is a tendency for most storm

summary statistics to attain greater values in winter months (June-August) than in summer months (December – February), although for wave direction this pattern is phase-shifted by a few months (Figure 4). In addition, seasonality is observed in the annually periodic MSL component (defined above using the time-series decomposition) which ranges over approximately 10 cm throughout the year, with the same pattern of higher values in winter months and lower values in summer months (Davies et al., submitted).

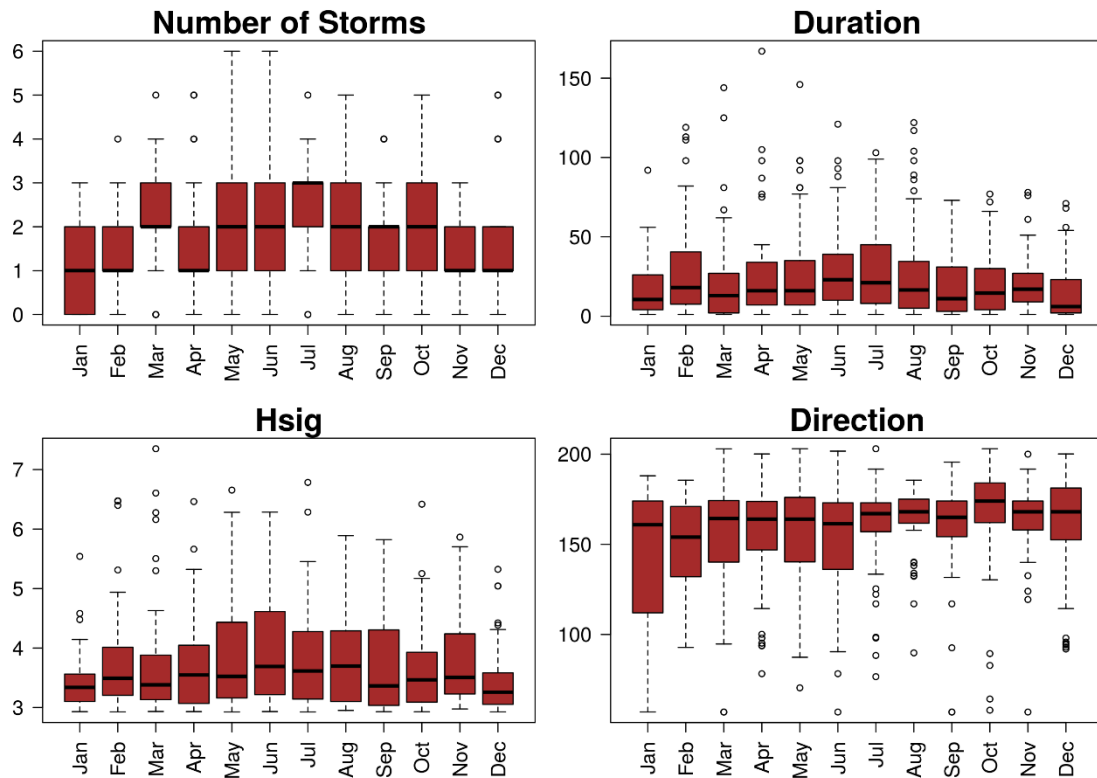


Figure 4: Monthly boxplots of the Old Bar storm summary statistics, which illustrate some of the seasonal non-stationarities in the data. There are clear winter increases in the number of storms each month as well as in the upper quantiles of the storm duration and H_{sig} . Other storm summary statistics show similar patterns (not shown), although for wave direction (bottom right) this trend appears phase-shifted, with more easterly storm directions from January to June as compared with July to December.

A number of the storm summary statistics also exhibit relations with the annually averaged southern oscillation index (herein denoted A_SOI), which we use as a proxy of ENSO (see also You and Jayewardene, 2003; You and Lord, 2008; Harley et al., 2010). Higher positive values of A_SOI are typically associated with La Nina climatic conditions, whereas lower negative values of A_SOI are typically associated with El Nino conditions. Relationships between storm summary statistics and A_SOI are most prominent for the wave direction and the smooth inter-annual MSL trend, both of which show a statistically significant correlation with A_SOI (Figure 5). In general there are more storm events from an easterly type direction during years with high A_SOI , which leads to a reduction in the annually averaged mean storm wave direction (Figure 5). The smooth inter-annual MSL also tends to be higher in years with high positive A_SOI (Figure 5), even after accounting for a background rise in MSL between 1985 and 2016

(Davies et al., submitted). There also appears to be a positive relationship between the annual number of storm events and the corresponding A_SOI value (Spearman rank correlation = 0.37 with 95% CI [0.02, 0.66]). We do not find clear relationships between A_SOI and other storm variables in this dataset, which may reflect either that there are no such relationships, or that they are not strong enough to be detected with our sample size (~30 years).

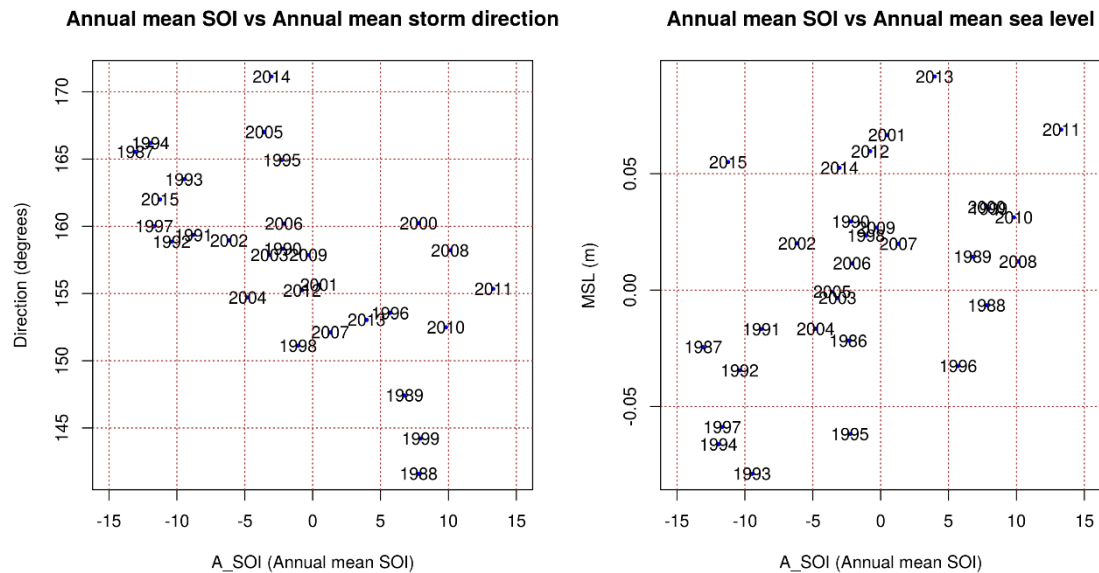


Figure 5: (Left) Annual mean storm direction versus Annual mean SOI (A_SOI) in the Old Bar storm summary statistics. (Right) Annual mean sea level versus Annual mean SOI (A_SOI).

To elucidate the magnitude of these effects, we discuss differences in the storm summary statistics during 'La Nina type years' (defined as years with $A_SOI > 5$) as compared with 'El Nino type years' (defined as years having $A_SOI < -5$). Our dataset has 8 years in each of these categories, although wave direction observations are only sufficiently complete in 7 of the 'El Nino type years'. The 'La Nina type years' have on average 4 storm events per year in the easterly sector (defined as events with wave directions north of 120 degrees), whereas during 'El Nino type years' there are less than half as many on average (1.7/year). Further, the smooth inter-annual MSL component is on average ~ 5cm higher in 'La Nina type years' than in 'El Nino type years'. In terms of the frequency of storms, there is an average of 24.75 storm events occurring in 'La Nina type years' compared with 21.375 during 'El Nino type years'.

The above analysis suggests that compared with 'El Nino type years', 'La Nina type years' have a substantial increase in the rate of storms in the easterly sector (about twice as many), and a moderate increase in the overall rate of storms (~15%) and the smooth inter-annual MSL component (~5cm). The impact of seasonal non-stationarities is more ubiquitous in this dataset, with most storm summary statistics showing an increase in winter as compared with summer (Figure 4). In the following section, we discuss the inclusion of these non-stationarities in a probabilistic model of the storm wave climate, which is designed to provide wave inputs to a shoreline evolution model as part of an erosion hazard assessment for Old Bar.

Probabilistic modelling of storm wave clustering

The statistical modelling framework outlined here enables seasonal and ENSO related non-stationarities to be included in the probabilistic coastal storm wave model. It involves the following key steps:

- 1) Modelling the storm event timings. The aim is to simulate a synthetic time-series of storm events which realistically captures the (seasonally and ENSO dependent) rate of storms, and the distribution of the time between storms. Qualitatively, the latter requirement implies realistic simulation of both closely spaced storm sequences (storm clusters), and of unusually large gaps between storms (quiescent periods).
- 2) Modelling the distributions of all storm summary statistics $\{H_{sig}, D, R, T, \theta\}$, including their dependence on the time of year and the annually averaged SOI (A_SOI). The aim is to ensure that the model simulates synthetic storms with summary statistics distributed similarly to the data, while also allowing for reasonable extrapolation beyond the range of the data where required (e.g. so that reasonable estimates of the 1/100 Annual Exceedance Probability H_{sig} or R are produced).
- 3) Modelling dependence in the joint distribution of all storm summary statistics. This is required to correctly simulate key physical relationships among storm variables, such as the tendency for storms with high H_{sig} to have (on average) longer duration D and higher surge R , and the tendency for storms with high H_{sig} to have longer wave period T due to limitations on wave steepness (Callaghan et al., 2008).
- 4) Simulating a long synthetic time-series of storm event sequences from the fitted models from Steps 1-3. This includes statistical simulation of future MSL and A_SOI (Davies et al., submitted). Synthetic storm event time-series enable the fitted model to be combined with shoreline evolution models for coastal erosion hazard applications (e.g. Callaghan et al., 2013).
- 5) Quantifying uncertainties in the fitted model. Fitting the statistical model involves estimation of parameters from limited data, and this inevitably introduces additional uncertainties into the predictions. When quantified, such uncertainties may translate into large uncertainties in estimated coastal erosion return periods (Callaghan et al., 2013). The magnitude of these uncertainties could have a substantial impact on how the results are optimally used in a coastal management context, so it is essential that uncertainties in the fitted model can be realistically quantified.

For brevity, herein we give a high level discussion of Steps 1 and 2 only. Full details of the above framework will be reported in a forthcoming publication (Davies et al., submitted). The steps discussed below involve modelling the dependence of the storm properties on seasonal and ENSO cycles, and are thus fundamental for integrating such non-stationarities into coastal erosion hazard assessments.

Step 1: Modelling the storm event timings

Our approach is a modification of that used by Callaghan et al. (2008), and involves modelling the storm event times as a non-homogeneous Poisson process, with additional constraints to prevent storm overlap. The mean storm arrival rate was modelled as being (possibly) dependent on covariates, including some periodic function of the time of year, and the annually averaged SOI (A_SOI). Sixteen different variations on the storm arrival rate model were fit to the observed storm event timings in our data, using maximum

likelihood to estimate the model parameters. These sixteen models cover cases with and without seasonal and ENSO dependence, as well as a range of parametric forms of the seasonal dependence (all of which are annually periodic functions of time). The Akaike Information Criterion (Bolker, 2008) was used to select the most parsimonious among the sixteen models. The most parsimonious model included an annually periodic saw-tooth seasonal component, and a positive dependence of the storm rate on the A_SOI value (Figure 6). It gave a reasonable representation of the observed seasonally dependent storm rate, with the annual rate of storms increasing by about 0.24 for each unit increase in A_SOI . The model also well simulated the observed distribution of times between storm events (Figure 6). This will be important for applications which are sensitive to the occurrence of storm clusters, or other details regarding the duration of inter-storm periods.

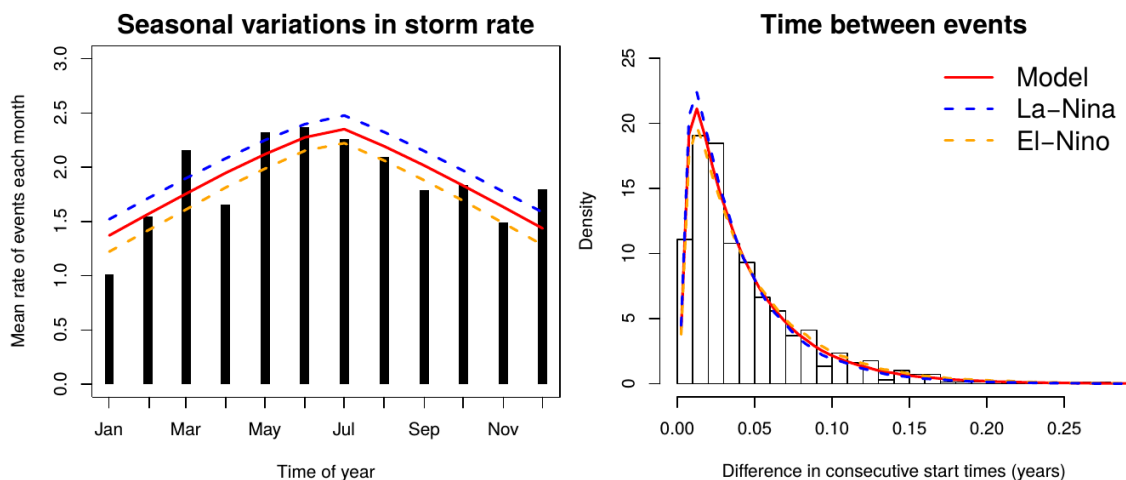


Figure 6: Modelled and observed storm event timings for Old Bar. (Left) Mean rate of storms each month, with black bars showing the observational data (30 years) and lines giving the modelled rates. The El Nino and La Nina curves give the modelled rates integrated over years with $A_SOI < -5$ and $A_SOI > 5$ respectively. (Right) Distribution of the time between consecutive storm events (in years). Bars depict the empirical data density, while the lines give the model results.

Step 2: Modelling the distributions of all storm summary statistics, including seasonal and ENSO dependence.

Initially we model the cumulative distribution functions of each storm summary statistic $\{H_{sig}, D, R, S, \theta\}$ separately, ignoring their seasonal or ENSO dependence. The storm wave steepness $S = H_{sig}/L$ was modelled in place of the storm wave period T . Here L is the wavelength, and S can be computed from observed values of T and H_{sig} using the Airy wave dispersion relation (Komar, 1998). If required, simulated values of T can be similarly back-calculated from simulated values of H_{sig} and S . We chose to model S instead of T because, for our dataset, direct modelling of wave steepness facilitated better representation of relationships between H_{sig} and T caused by limitations in wave steepness (Davies et al., submitted).

Extreme value mixture models (Scarrot, 2015) were used to model the distributions of those storm summary statistics for which extremes are of importance for coastal erosion modelling, namely H_{sig} , D , and R . For the latter variables the use of parametric distributions is essential, at least to model the upper tail, because for erosion hazard applications we need to extrapolate beyond the range of the observed data (e.g. to

account for the 1/100 AEP storm H_{sig} , which is unlikely to have been observed in 30 years of data). These parametric extreme value mixture models were fit to the data with maximum likelihood. For other storm variables (θ and S) we fit smooth empirical distribution functions to the data, using with the logspline method of Kooperberg and Stone (1992).

To account for seasonal dependence in the fitted distributions, for each of the above storm variables $\{H_{sig}, D, S, R, \theta\}$ we used an Archimedian copula to model its joint distribution with a seasonal variable. The latter seasonal variable is defined (separately for each storm variable) as $\cos(2\pi(t - \varphi))$ where t is the storm start time in years, and φ is uniquely set for each storm variable to the value which gives the strongest (negative) rank correlation between the seasonal and storm variables. This choice of φ helps to emphasise the seasonality in the modelled joint distribution, because using copulas we can model the joint distribution of the storm and seasonal variables in a way which ‘well represents’ rank based relations between them. Once the joint distribution has been fit, it is straightforward to derive the distribution of the storm variable conditional on the seasonal variable. Using this approach the simulated H_{sig} distribution (Figure 7) shows a similar seasonal pattern to the data (Figure 4), with a winter maxima and summer minima.

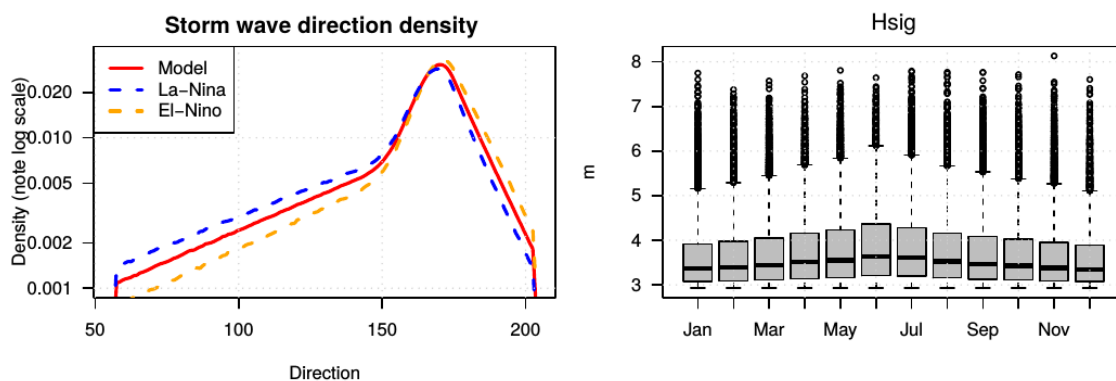


Figure 7: Examples of non-stationarities in the modelled storm summary statistics for Old Bar. (Left) Probability density of modelled storm wave direction. To illustrate the impact of ENSO we also report the results restricted to ‘La Nina type years’ with the modelled $A_{SOI} > 5$, and ‘El Nino type years’ with the modelled $A_{SOI} < -5$; (Right) Seasonal variation in the H_{sig} distribution. Note the overall increase in quantiles during winter (mid-year). The plot is based on a long synthetic time-series generated from the best-fit model, so there is some stochasticity in the upper tails of the boxplots.

In the case of storm wave direction θ , we employ related copula-based techniques derive the distribution of θ conditional on the ENSO proxy A_{SOI} , as well as on the seasonal variable. Full details will be reported in a forthcoming publication (Davies et al., Submitted). The fitted model captures the easterly shift in the storm direction distribution which occurs during ‘La Nina type years’ as compared with ‘El Nino type years’ (Figure 7). When combined with the storm rate model described above, the model predicts an average of 2.05 ([1.48, 2.79] 95% CI) storms in the easterly sector (north of 120 degrees) during ‘El Nino type years’, compared with an average of 3.90 ([2.91, 4.98] 95% CI) events during ‘La Nina type years’. This is in good agreement with direct estimates from the data, which gave an average of 1.7 and 4.0 such events in ‘El Nino type years’ and ‘La Nina type years’ respectively.

Summary and Conclusions

Probabilistic coastal erosion hazard assessments may be developed by forcing deterministic shoreline evolution models with probabilistic storm event models. ENSO and seasonal cycles may have a significant influence on coastal erosion hazards, and so it is desirable to be able to include such non-stationarities in probabilistic erosion hazard assessments. To enable this, we have developed a framework for probabilistic modelling of synthetic storm events, which realistically simulates the temporal sequencing of storms (e.g. storm clustering) and includes the impact of ENSO and seasonal non-stationarities on storm properties. The modelling framework is quite general and adaptable to other sites and other types of non-stationarities affecting the storm wave climate, so long as sufficient data is available to estimate the statistical model parameters. Uncertainties in the latter parameters can be quantified and propagated through to uncertainties in the modelled storm wave climate, and into coastal erosion predictions. The framework has been applied to a historical wave time-series relevant to Old Bar, NSW, following an exploratory data analysis which suggests both ENSO and seasonality influence the storm wave climate. The model shows good capacity to represent the observed statistical properties of storm events. Ongoing work is applying the modelled storm series for Old Bar to site-specific shoreline response modelling to better understand the cumulative impact of storms on an eroding coast.

Acknowledgements

This paper was published with the permission of the CEO, Geoscience Australia. Wave and tidal data were provided by the Manly Hydraulics Laboratory. This research forms part of the Bushfire and Natural Hazards CRC project 'Resilience to clustered disaster events on the coast – Storm Surge'.

References

- Barnard, P.L., Short, A.D., Harley, M.D., Splinter, K.D., Vitousek, S., Turner, I.L., Allan, J., Banno, M., Bryan, K.R., Doria, A., Hansen, J.E., Kato, S., Kuriyama, Y., Randall-Goodwin, E., Ruggiero, P., Walker, I.J. and Heathfield, D.K., 2015. Coastal vulnerability across the pacific dominated by el nino/southern oscillation. *Nature Geoscience*, 8:801-807
- Bolker, B.M., 2008. *Ecological models and data in R*. Princeton University Press, Princeton, 409 pp.
- Callaghan, D. P., Nielsen, P., Short, A., and Ranasinghe, R., 2008. Statistical simulation of wave climate and extreme beach erosion. *Coastal Engineering* 55, 375-390
- Callaghan, D. P., Ranasinghe, R. and Roelvink, D., 2013. Probabilistic estimation of storm erosion using analytical, semi-empirical and process based storm erosion models. *Coastal Engineering* 82, 64-75
- Coco, G., Senechal, N., Rejas, A., Bryan, K. R., Capo, S., Parisot, J. P., Brown, J. A. and MacMahan, J. H. M., 2014. Beach response to a sequence of extreme storms. *Geomorphology*, 204: 493-501.

- Corbella, S. and Stretch, D.D., 2012. Multivariate return periods of sea storms for coastal erosion risk assessment. *Natural Hazards and Earth System Sciences*, 12(8): 2699-2708.
- Cowell, P. J., Thom, B. G., Jones, R. A., Everts, C. H. and Simanovic, D. (2006) Management of Uncertainty in Predicting Climate-Change Impacts on Beaches. *Journal of Coastal Research* 221, 232-345
- Cleveland, R.B., Cleveland, W.S., McRae, J.E. and Terpenning, I., 1990. STL: A seasonal-trend decomposition procedure based on loess. *Journal of Official Statistics*, 6(1): 3-73
- Davies, G., Callaghan, D. P., Gravios, U., Jiang, W., Hanslow, D. J., Nichol, S., Baldock, T. (Submitted Manuscript) Improved treatment of non-stationary conditions and uncertainties in probabilistic models of storm wave climate.
- Dissanayake, P., Brown, J., Wisse, P. and Karunaratna, H., 2015. Effects of storm clustering on beach/dune evolution. *Marine Geology*, 370: 63-75.
- Egbert, G.D. and Erofeeva, S.Y., 2002. Efficient inverse modeling of barotropic ocean tides. *Journal of Atmospheric and Oceanic Technology*, 19(2): 183-204.
- Ferreira, Ó., 2005. Storm groups versus extreme single storms: Predicted erosion and management consequences. *Journal of Coastal Research*: 221-227.
- Hanslow, D. J., Dela-Cruz, J., Morris, B. D., Kinsela, M., Foulsham, E., Linklater, M., and Pritchard, T. R. (2016) Regional scale coastal mapping to underpin strategic land use planning in southeast Australia. *Journal of Coastal Research* SI75, 987-991
- Harley, M.D., Turner, I.L., Short, A.D. and Ranasinghe, R., 2010. Interannual variability and controls of the Sydney wave climate. *International Journal of Climatology*, 30(9): 1322-1335.
- Harley, M.D., Turner, I.L., Short, A.D. and Ranasinghe, R., 2011. A re-evaluation of coastal embayment rotation: The dominance of cross-shore versus alongshore sediment transport processes, Collaroy-Narrabeen beach, southeast Australia. *Journal of Geophysical Research*, 116(F4): F04033
- Kinsela, M. A. and Hanslow, D. J. 2013. Coastal Erosion Risk Assessment in New South Wales: Limitations and Potential Future Directions. *NSW Coastal Conference 2013*.
- Kinsela, M. A., Morris, B. D., Daley, M. J. A., and Hanslow, D. J., 2016. A Flexible Approach to Forecasting Coastline Change on Wave-Dominated Beaches. *Journal of Coastal Research* SI75, 952-956
- Komar, P.D. 1998. Beach processes and sedimentation. Second Edition. Prentice-Hall, New Jersey.
- Kooperberg, C. and Stone, C.J., 1992. Logspline density estimation for censored data. *Journal of Computational and Graphical Statistics*, 1(4): 301-328.
- Kulmar, M. A., 1995. Wave direction distributions off Sydney, New South Wales. *Proceedings 12th Australasian Conference on Coastal and Ocean Engineering, Melbourne*. 175-181
- Kulmar, M. A., Modra, B., and Fitzhenry, M., 2013. The New South Wales Wave Climate: Improved Understanding through the Introduction of Directional Wave Monitoring Buoys. *Proceedings of Coasts and Ports 2013, Sydney, Australia*.

- Li, F., van Gelder, P.H.A.J.M., Vrijling, J.K., Callaghan, D.P., Jongejan, R.B. and Ranasinghe, R., 2014. Probabilistic estimation of coastal dune erosion and recession by statistical simulation of storm events. *Applied Ocean Research*, 47, 53-62.
- Li, F., van Gelder, P.H.A.J.M., Ranasinghe, R., Callaghan, D.P. and Jongejan, R.B., 2014b. Probabilistic modelling of extreme storms along the Dutch coast. *Coastal Engineering*, 86, 1-13.
- de Michele, C., Salvadori, G., Passoni, G. and Vezzoli, R., 2007. A multivariate model of sea storms using copulas. *Coastal Engineering*, 54(10): 734-751.
- Nichol, S. L., McPherson, A., Davies, G., Jiang, W., Howard, F., Gravois, U., Callaghan, D., and Baldock, T., 2016. A Framework for Modelling Shoreline Response to Clustered Storm Events: A Case Study from Southeast Australia. *Journal of Coastal Research* SI75, 1197-1201
- Ranasinghe, R., McLoughlin, R., Short, A. and Symonds, G., 2004. The southern oscillation index, wave climate, and beach rotation. *Marine Geology*, 204(3-4), 273-287.
- Ranasinghe, R., Callaghan, D.P. and Stive, M.J.F., 2012. Estimating coastal recession due to sea level rise: Beyond the Bruun rule. *Climatic Change*, 110, 561–574.
- Serafin, K. A. and Ruggiero, P., 2014. Simulating extreme total water levels using a time-dependent, extreme value approach. *Journal of Geophysical Research: Oceans*, 119(9): 6305-6329.
- Southgate, H.N., 1995. The effects of wave chronology on medium and long term coastal morphology, *Coastal Engineering*, Volume 26, Issues 3-4, December 1995, Pages 251-270.
- Thom, B.G 1974 Coastal Erosion in Eastern Australia. *Search* Vol5, No5 198-208.
- You, Y.G. and Jayewardene, I., 2003. Prediction of the occurrence of extreme coastal storms along the NSW coast. *National Environment Conference*, Brisbane, 5 (on CD)
- You, Y.G. and Lord, D., 2008. Influence of the el niño southern oscillation on the NSW coastal storm severity. *Journal of Coastal Research*, 24, 203-207
- Wainwright, D.J., Ranasinghe, R., Callaghan, D.P., Woodroffe, C.D., Jongejan, R., Dougherty, A.J., Rogers, K. and Cowell, P.J., 2015. Moving from deterministic towards probabilistic coastal hazard and risk assessment: Development of a modelling framework and application to Narrabeen beach, New South Wales, Australia. *Coastal Engineering*, 96, 92-99.